Stability and nonlinear dynamics of solitary waves generated by subcritical oscillatory instability under the action of feedback control

Y. Kanevsky and A. A. Nepomnyashchy
Department of Mathematics, Technion-Israel Institute of Technology, Haifa 32000, Israel
(Received 5 August 2007; published 10 December 2007)

We consider the influence of global feedback control which acts on an oscillatory system governed by a subcritical Ginzburg-Landau equation. Exact solutions corresponding to solitary-wave solutions are obtained. A generalized variational approach is applied for the simplification of the whole problem and its reduction to a finite-dimensional dynamical model. The finite-dimensional evolution model is used for studying the indirect interaction between solitary waves caused by the global control. The stability analysis is held in the framework of the finite-dimensional model. The boundaries of monotonic and oscillatory instabilities are obtained. The basic types of dynamics provided by the finite-dimensional model are described and compared with the results of a direct numerical simulation of the original equation.

DOI: 10.1103/PhysRevE.76.066305 PACS number(s): 47.54.−r, 82.40.Bj, 89.75.Kd

I. INTRODUCTION

One of the subjects that recently started attracting the growing attention of researchers working in the area of nonlinear dynamics and pattern formation is an active feedback control of pattern forming systems. The aim of feedback control is to achieve the desirable dynamics or a particular pattern. It has been applied to Rayleigh-Bénard convection [1,2], Marangoni convection [3–5], contact line instability in thin liquid films [6–8], catalytic reactions [9–12], and crystal growth [13]. The effect of feedback control of supercritical oscillatory instabilities was investigated in Refs. [12,14–20]. Feedback control of subcritical oscillatory instabilities has hardly been investigated. The possibility of the suppression of a subcritical oscillatory instability by means of feedback control has been demonstrated in Ref. [21]. Numerical simulations in Ref. [21] have revealed various regimes of the solution dynamics: a single stationary pulse, coexistence of several pulses, competition of pulses, chaotic short pulses, and synchronized pulses.

In the present paper, we explain some of obtained results by means of a finite-dimensional model of nonlinear evolution equations which are derived using an analytical approach, based on the variational principle. In Sec. II, we discuss the basic equation and its localized solutions. In Sec. III we consider the variational approach and the method of moments and derive the finite-dimensional dynamical system which is used for modeling the behavior of the original system. The stability test of stationary solutions and description of results are provided in Sec. IV. Section V contains concluding remarks.

II. MATHEMATICAL MODEL

We consider the subcritical complex Ginzburg-Landau equation (CGLE) under a feedback control

$$A_t = A + (1+ib)A_{xx} - (-1+ic)|A|^2 A + K(A)A. \tag{1}$$

Feedback control is imposed by adding a term $K(A)A$ to the right-hand side of Eq. (1), with a control functional $K(A)$ of the form (see Refs. [13,21]):

$$K(A) = -p \max_x |A|. \tag{2}$$

Solutions can be presented in the form

$$A(x,t) = R(x,t)e^{i\theta(x,t)}, \tag{3}$$

where $R(x,t)$ and $\theta(x,t)$ are real functions, and thus the control functional can be written as $K(A)=-p \max R$. Substituting Eq. (3) into the Eq. (1) and denoting $\max_x R \equiv R_{\max}$, we obtain the following system of two real equations:

$$R_t = R_{xx} - R\theta_x^2 - b(2\theta_x R_x + R\theta_{xx}) + R^3 + (1 - pR_{\max})R,$$

$$R\theta_t = b(R_{xx} - R\theta_x^2) + (2\theta_x R_x + R\theta_{xx}) - cR^3. \tag{4}$$

Note that the parameter $\mu = 1 - pR_{\max}$ is the effective linear growth rate parameter.

The system of Eqs. (4) has the following exact pulse solutions:

$$R(x,t) = \frac{C}{\cosh \kappa x}, \quad \theta(x,t) = \gamma \ln \cosh \kappa x - \Omega t, \tag{5}$$

where

$$C = \frac{p}{2(1-\alpha)}[1 \pm \sqrt{1 - 4(1-\alpha)/p^2}] > 0,$$

$$\alpha = \frac{1}{12(1+b^2)}[\sqrt{9(bc-1)^2 + 8(b+c)^2} - 3(bc-1) + 4b(b+c)],$$

$$\gamma = \frac{1}{b+c}[6\alpha(1+b^2) + 3(bc-1) - 2b(b+c)],$$

$$\kappa^2 = C^2 \frac{1}{3\gamma}\frac{b+c}{1+b^2}, \quad \Omega = b\kappa^2 - \gamma\kappa^2 + cC^2. \tag{6}$$

Solution (6) is identical to the pulse solution of a noncontrolled subcritical CGLE

 ©2007 The American Physical Society

$$A_t = \mu A + (1+ib)A_{xx} - (-1+ic)|A|^2 A, \tag{7}$$

with $\mu = 1 - pC$. Such solutions have been known for a long time [22–25], but typically they are unstable and blow up in finite time, which corresponds to the transition to a strongly nonlinear dynamics beyond the applicability of CGLE. The goal of the present paper is to clarify whether global feedback control described by Eqs. (1) and (2), which can also be written as

$$A_t = (1-pC)A + (1+ib)A_{xx} - (-1+ic)|A|^2 A + p(C - \max_x |A|)A, \tag{8}$$

can suppress blow up and stabilize a pulse solution.

For $\alpha < 1$ the two solutions for C exist for $p > 2\sqrt{1-\alpha}$ and the linear growth rate $\mu = 1 - pC < 0$. Therefore, the solutions can be stable in this region of parameters, or, in other notation, for $\{-b - 3\sqrt{b^2+1} < c < -b + 3\sqrt{b^2+1}\}$. The stability of pulse solutions will be discussed in more detail in Sec. IV.

For $\alpha > 1$, i.e., for $c > -b + 3\sqrt{b^2+1}$ or for $c < -b - 3\sqrt{b^2+1}$, there is only one solution for $C > 0$ and there holds $\mu = 1 - pC > 0$. Because μ is the effective linear growth rate, the solution (5) is obviously unstable with respect to disturbances that do not decay as $x \to \pm\infty$.

In this case, it is interesting to investigate the nonlinear dynamics produced by the instability of pulse solutions. In Ref. [21], the problem was studied by means of a direct numerical simulation of Eq. (1). A remarkable observation done in Ref. [21] is that in many cases the dynamic regime is determined by an indirect interaction of pulses through the applied feedback control. In a certain region of parameters, a coexistence of pulses leads to the development of multipulse regimes. In another region of parameters, the pulses compete, therefore only one pulse "rules" for some time, until it gets "overthrown" by another pulse. In the present paper we provide an explanation of these phenomena.

III. FINITE-DIMENSIONAL MODELS OF PULSE DYNAMICS

The analysis of the dependence of the dynamical regime on the parameters is simplified by means of a finite-dimensional model. In the case of a conservative system, the natural way of constructing a finite-dimensional dynamical model is based on the variational principle. This principle was developed for the investigation of the behavior of stable spatiotemporal solitons whose dynamics is governed by numerous Lagrangian modifications of the nonlinear Schrödinger equation used in nonlinear optics (see the review paper [26]). The variational approach is based on the approximation of solutions by a certain *Ansatz*, so that the Lagrangian functional becomes a function of a finite number of variables. The corresponding Euler equations serve as the finite-dimensional dynamical system modeling the original problem.

Unlike the conservative systems, the evolution equations which govern dissipative systems have no natural variational formulation. Nevertheless, two different approaches have been suggested in the literature for the derivation of the finite-dimensional dynamical models. The first approach is based on a modified variational technique. It has been applied in Ref. [27] for finding approximated solutions of the dissipative nonlinear Schrödinger equation. This technique was extended for the treatment of complex dissipative systems described by the cubic-quintic CGLE in Ref. [28].

Another approach, based on the computation of generalized moments, has been suggested in Ref. [29]. It has been applied for investigation of dynamics of solitons of the cubic-quintic CGLE using trial functions of different types for deriving various finite-dimensional evolutional models. Below we employ both approaches for the derivation of finite-dimensional models and compare the results.

A. Model I

The equations that are used for the treatment of complex dissipative systems are written in the following form:

$$F[u] = Q, \tag{9}$$

where $F[u]$ is a conservative part of Eq. (9), that is, there exists a Lagrangian $L[u, u^*]$ such that

$$\left(\frac{\delta L}{\delta u}\right)^* = \frac{\delta L}{\delta u^*} = F[u] \tag{10}$$

and Q is a nonconservative part of Eq. (9). If one utilizes an *Ansatz* of the form

$$u = u(b_1(t), b_2(t), \ldots, b_N(t), x), \tag{11}$$

then the variational technique which is used in Ref. [27] can be represented by the following system of equations:

$$\frac{d}{dt}\frac{\partial \langle L\rangle}{\partial (b_j)_t} - \frac{\partial \langle L\rangle}{\partial b_j} = 2\,\mathrm{Re}\int_{-\infty}^{\infty} Q\frac{\partial u^*}{\partial b_j}dx, \quad j = 1, \ldots, N, \tag{12}$$

where

$$\langle L\rangle = \int_{-\infty}^{\infty} L[u(b_1(t), b_2(t), \ldots, b_N(t), x), u^*(b_1(t), b_2(t), \ldots, b_N(t), x)]dx. \tag{13}$$

We have applied the extended variational method to the Eq. (1), with a control functional of the form (2). Equation (1) can be written in the form

$$iA_t + bA_{xx} - c|A|^2 A = i\{[1 - K(A)]A + A_{xx} + |A|^2 A\}. \tag{14}$$

The right-hand side of Eq. (14) is the nonconservative part Q. The Lagrangian of the left-hand side of Eq. (14) is as follows:

$$L = \frac{i}{2}(AA_t^* - A^* A_t) + b|A_x|^2 + \frac{c}{2}|A|^4. \tag{15}$$

For studying the dynamics of a one-pulse solution, we use the *Ansatz* compatible with the exact pulse solution (5)

$$R(x,t) = \frac{C(t)}{\cosh[\kappa(t)x]}, \quad \theta(x,t) = \gamma(t)\ln\cosh[\kappa(t)x] + \phi(t), \tag{16}$$

with $C(t)$, $\kappa(t)$, $\gamma(t)$, and $\phi(t)$ playing the role of $b_1(t),\ldots,b_4(t)$. In this case the control functional can be written in the form $K(A)=-pC$. The obtained evolution equations for $C(t)$, $\kappa(t)$, $\gamma(t)$, and $\phi(t)$ are as follows:

$$C_t = \frac{1}{9}C[9 - 9pC + 8C^2 - (\gamma^2 + 6b\gamma + 7)\kappa^2],$$

$$\kappa_t = \frac{4}{9}\kappa[C^2 - (3b\gamma + 2 - \gamma^2)\kappa^2],$$

$$\gamma_t = \frac{2}{3}C^2(c - \gamma) + \frac{2}{3}\kappa^2(2b - \gamma)(1 + \gamma^2),$$

$$\phi_t = -\frac{1}{9}C^2[6\ln 2(\gamma - c) - 4(\gamma - 3c)] + \frac{1}{9}\kappa^2[(6\ln 2 - 4)(2b - \gamma)(1 + \gamma^2) - 7b] - b\gamma^2 + 6\gamma. \tag{17}$$

According to definitions, $C(t)$ and $\kappa(t)$ are non-negative.

For the investigation of the interaction of two distant pulselike solutions, we use the *Ansatz* $A=A_1+A_2$, $A_j = R_j \exp[i\theta_j]$, where

$$R_j(x,t) = \frac{C_j(t)}{\cosh[\kappa_j(t)(x - x_j)]},$$

$$\theta_j(x,t) = \gamma_j(t)\ln\cosh[\kappa_j(t)(x - x_j)] + \phi_j(t), \quad j = 1,2 \tag{18}$$

for each of the solitary waves, which leads to the following variational model (the overlap of solitary waves is disregarded):

$$\dot{C}_1 = \frac{1}{9}C_1[9 - 9p\ \max\{C_1,C_2\} + 8C_1^2 - (\gamma_1^2 + 6b\gamma_1 + 7)\kappa_1^2],$$

$$\dot{\kappa}_1 = \frac{4}{9}\kappa_1[C_1^2 - (3b\gamma_1 + 2 - \gamma_1^2)\kappa_1^2],$$

$$\dot{\gamma}_1 = \frac{2}{3}C_1^2(c - \gamma_1) + \frac{2}{3}\kappa_1^2(2b - \gamma_1)(1 + \gamma_1^2),$$

$$\dot{C}_2 = \frac{1}{9}C_2[9 - 9p\ \max\{C_1,C_2\} + 8C_2^2 - (\gamma_2^2 + 6b\gamma_2 + 7)\kappa_2^2],$$

$$\dot{\kappa}_2 = \frac{4}{9}\kappa_2[C_2^2 - (3b\gamma_2 + 2 - \gamma_2^2)\kappa_2^2],$$

$$\dot{\gamma}_2 = \frac{2}{3}C_2^2(c - \gamma_2) + \frac{2}{3}\kappa_2^2(2b - \gamma_2)(1 + \gamma_2^2). \tag{19}$$

Equations for $\dot{\phi}_j$ do not influence the dynamics and are not written here.

B. Model II

We have also used the method of moments developed in Ref. [29]. This method also represents a reduction of a complete problem to a finite-dimensional dynamical model. For an arbitrary localized field, integrals of energy, momentum and higher-order generalized moments are introduced. For a certain *Ansatz* these integrals become functions of several parameters. The number of the higher-order generalized moments is, in general, infinite, but it is restricted to a finite number in order to obtain the simplified model. Further, the algebraic combinations and the integration of the original equation lead to the derivation of the evolution equations for the generalized moments, the details see in Ref. [29], and references therein.

The application of the method of moments to Eq. (1) provides a model that is similar in its structure to the variational model (17) but slightly differs in the constant coefficients. The obtained evolution equations for $C(t)$, $\kappa(t)$, $\gamma(t)$, and $\phi(t)$ are as follows:

$$C_t = \frac{1}{\pi^2}C\left\{\pi^2 - \pi^2 pC + \left(2 + \frac{2\pi^2}{3}\right)C^2 - \left[\left(\frac{\pi^2}{3} - 2\right)\gamma^2 + 6b\gamma + 4 + \frac{\pi^2}{3}\right]\kappa^2\right\},$$

$$\kappa_t = \frac{4}{\pi^2}\kappa[C^2 - (3b\gamma + 2 - \gamma^2)\kappa^2],$$

$$\gamma_t = \frac{2}{3}C^2(c - \gamma) + \frac{2}{3}\kappa^2(2b - \gamma)(1 + \gamma^2),$$

$$\phi_t = -\frac{1}{9}C^2\left\{6\ln 2(\gamma - c) - 4\left[\left(\frac{3}{2} - \frac{9}{2\pi^2}\right)\gamma - 3c\right]\right\} + \frac{1}{9}\kappa^2\left[(6\ln 2 - 4)(2b - \gamma)(1 + \gamma^2) - 7b - \left(7 - \frac{54}{\pi^2}\right)b\gamma^2 + \left(2 + \frac{36}{\pi^2}\right)\gamma + \left(2 - \frac{18}{\pi^2}\right)\gamma^3\right]. \tag{20}$$

Note, that if π^2 is replaced by 9, then the system of Eqs. (20) converts to the model (17). Furthermore, the stationary points for models (17) and (20) are the same (details are presented in the next section).

In order to further compare both approaches, we have applied the variational method of Sec. III A to the cubic-quintic CGLE using one of the *Ansätze* from Ref. [29], and we found that the obtained evolution equations were absolutely identical to those obtained in Ref. [29]. Thus, we conclude that both approaches are compatible, and lead to very close systems, hence there is no need in a special investiga-

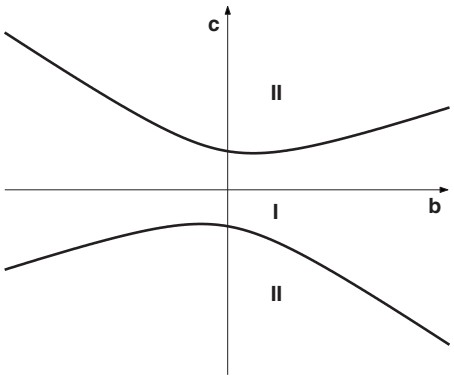

FIG. 1. The (b,c) plane. I: the region with $1-pC<0$, II: the region with $1-pC>0$. Solid lines: the boundary $1-pC=0$.

tion of the dynamics described by each of the models. Later on, we concentrate our attention on the models (17) and (19) obtained by means of the variational approach.

IV. NONLINEAR DYNAMICS

In the present section, we consider the stability of pulse solutions (5) and (6) in the framework of the finite-dimensional dynamical models (17) and (19), and the dynamical regimes caused by their instabilities.

A. Stationary solutions

First, let us consider stationary points of the model (17) which are obtained by letting $C_t=\kappa_t=\gamma_t=0$ and $\phi_t=-\Omega$ (recall that C and κ are chosen non-negative). The exact solution (6) is reproduced. As was mentioned above, for $\alpha<1$ the two solutions for C exist for $p>2\sqrt{1-\alpha}$ and the linear growth rate $\mu=1-pC<0$. For $\alpha>1$ there is only one solution for C and there holds $\mu=1-pC>0$. The condition $1-pC=0$ is equivalent to conditions $c=-b\pm 3\sqrt{b^2+1}$ in the plane of parameters b and c, see Fig. 1. Due to the symmetry regarding the origin, we can consider only the upper half-plane of the parameters.

When the model (19) is used, we obtain four kinds of nontrivial stationary solutions $u_j=(C_j,\kappa_j,\gamma_j)$, $j=1,2$: (i) $C_1\neq 0$, $C_2=0$ which leads to a solution $u_1=(C,\kappa,\gamma)$, $u_2=(0,0,\gamma_2)$, where C,κ,γ are given by Eq. (6) and γ_2 is arbitrary; (ii) $C_1=0$, $C_2\neq 0$ which leads to a solution $u_1=(0,0,\gamma_1)$, $u_2=(C,\kappa,\gamma)$, where C,κ,γ are given by Eq. (6) and γ_1 is arbitrary; (iii) $u_1=u_2=(C,\kappa,\gamma)$, where C,κ,γ are given by Eq. (6); (iv) on the line $\alpha=1$ (or $pC=1$), two more families of stationary solutions exist: the first family is $u_1=(C,\kappa,\gamma)$, $u_2=(C_2,\kappa_2,\gamma)$, where C_2 is an arbitrary number satisfying the condition $0<C_2<C$ and $\kappa_2=C_2/\sqrt{1+b\gamma}$ and the second one is $u_1=(C_1,\kappa_1,\gamma)$, $u_2=(C,\kappa,\gamma)$, $0<C_1<C$, and $\kappa_1=C_1/\sqrt{1+b\gamma}$. We shall call solutions of types (i) and (ii) single-pulse solutions, solutions of type (iii) two-pulse solutions, and solutions of type (iv) mixed-mode solutions. Below we consider the stability of stationary solutions.

B. Coexistence and competition of pulses

We start with the consideration of monotonic instabilities of pulses.

1. Stability of the pulse to the disturbances of its shape

In order to investigate the internal stability of the pulse solution, we linearized the system (17) around the solution (6). The linear growth rate of the perturbed solution λ is a solution of the following characteristic equation:

$$\lambda^3+a_1\lambda^2+a_2\lambda+a_3=0, \tag{21}$$

where

$$a_1=\frac{1}{9}[C(9p-16C)+2\kappa^2(2\gamma^2+9b\gamma+17)], \tag{22}$$

$$a_2=\frac{2}{81}\kappa^2[C(9p-16C)(2\gamma^2+9b\gamma+17)+4\kappa^2(64+18b^2+11\gamma^2+36b^2\gamma^2+69b\gamma+\gamma^4-3b\gamma^3)],$$

$$a_3=\frac{16}{9}\kappa^4(1+b^2)(2+\gamma^2)(2-pC). \tag{22}$$

The monotonic instability boundary $\lambda=0$ is equivalent to a condition $a_3=0$, that is, to a condition $pC=2$. Therefore, it holds $\mu=1-pC=-1<0$, so we are in region I for which the existence condition is $p^2\geq 4(1-\alpha)$, where α is a function of b and c.

Next, solving the equation $pC=2$ leads to $p^2=4(1-\alpha)$. Thus, $\lambda=0$ holds for $p^2=4(1-\alpha)$ and this condition corresponds to one solution for C from Eq. (6). For $p^2>4(1-\alpha)$ there exist two solutions for C, $C_+=1/[2(1-\alpha)][p+\sqrt{p^2-4(1-\alpha)}]$ and $C_-=1/[2(1-\alpha)][p-\sqrt{p^2-4(1-\alpha)}]$. For the upper branch of solution $C=C_+$ it holds $pC>2$ and $a_3<0$, hence the product of the eigenvalues is positive and therefore at least one of the eigenvalues λ must be positive, thus the upper branch of C is unstable. For the lower branch of solution $C=C_-$ it holds $pC<2$ and $a_3>0$ therefore the product of the eigenvalues is negative and at least one eigenvalue is negative. Thus, the boundary $\lambda=0$ corresponds to a transition from one branch of solution to another.

Furthermore, from Eqs. (6) and (17) it follows that

$$8C^2=9pC-9+\kappa^2(\gamma^2+6b\gamma+7), \tag{23}$$

hence

$$a_1=2-pC+\frac{2}{9}\kappa^2(\gamma^2+3b\gamma+10). \tag{24}$$

From the equation for γ, $\gamma^2(b+c)-3\gamma(bc-1)-2(b+c)=0$, it follows that $3b\gamma+2>\gamma^2>0$, therefore $a_1>0$ for $pC\leq 2$. However, the coefficient a_2 changes its sign for certain values of b, c, and p, hence there is a possibility for a pulse solution to be unstable for $pC<2$.

For example, for $b=10$, $c=20$, and $p=0.25$, one can obtain that $a_2<0$, and the eigenvalues are approximately 16.73, 1.01, and −42.18. Thus, in the framework of the finite-dimensional model the solution with $C=C_-$ is unstable for abovementioned values of parameters. The direct simulation of Eq. (1) for the abovementioned values of parameters shows the blow-up of a pulse solution. With the increasing value of p we have obtained an oscillatory instability (for

example, for $p=0.8$ eigenvalues are approximately $0.2\pm1.2i$, -3.2) and then a stability (for example, for $p=2$ eigenvalues are approximately $-0.4\pm0.3i$, -0.5) of a pulse solution for $b=10$ and $c=20$.

Therefore, one can conclude that the possibility of instability can be suppressed by demanding some condition on p. For $pC\leq 2$ it holds $C\leq 2/p$ and therefore

$$a_2 \geq \frac{2}{81}\kappa^2[C(9p-32/p)\underbrace{(2\gamma^2+9b\gamma+17)}_{>0}+4\kappa^2 \times \underbrace{(64+18b^2+11\gamma^2+36b^2\gamma^2+69b\gamma+\gamma^4-3b\gamma^3)}_{>0}], \quad (25)$$

thus, for $p\geq 4\sqrt{2}/3$ it holds $a_2>0$, and the solution $C=C_-$ is stable in the whole region I.

We must mention that a condition $p\geq 4\sqrt{2}/3$ is fulfilled automatically for $\alpha\leq 1/9$, because for $\alpha\leq 1/9$ it holds that $2\sqrt{1-\alpha}\geq 4\sqrt{2}/3$, and $p\geq 2\sqrt{1-\alpha}$ is an existence condition. For $1/9<\alpha<1$ one can obtain a more precise condition on p, $p>16/3\sqrt{9\alpha+7}$, where $16/3\sqrt{9\alpha+7}<4\sqrt{2}/3$.

2. Stability of the pulse to the appearance of another pulse

The stability of the solution with regards to the appearance of the second soliton can be studied in the framework of the model (19). We linearize the system (19) around the solution (6) for A_1 and around a solution $(0,0,\gamma)$ for A_2. The linear growth rate of the perturbed solution, λ, is a solution of the following characteristic equation

$$\lambda^2(1-pC-\lambda)(\lambda^3+a_1\lambda^2+a_2\lambda+a_3)=0, \quad (26)$$

where a_1, a_2, a_3 are given by Eq. (22). The boundary $\lambda=0$ is equivalent to conditions $a_3=0$ or $1-pC=0$, that is, to conditions $pC=2$ or $pC=1$. The latter condition is equivalent to conditions $c=-b\pm 3\sqrt{1+b^2}$. Therefore, for $1-pC>0$ it holds $\lambda=1-pC>0$ and the single-pulse solution is unstable. For $1-pC<0$ it holds $\lambda=1-pC<0$ and the single-pulse solution is stable for $C=C_-$.

3. Stability of a two-pulse solution

The monotonic stability of a two-pulse solution can be studied by linearizing the system (19) around the solution (6) for both A_1 and A_2 and assuming a certain relation between the perturbations $\tilde{C}_1$, $\tilde{C}_2$, e.g., $\tilde{C}_1>\tilde{C}_2$. Then the characteristic equation is as follows:

$$(\lambda^3+a_1\lambda^2+a_2\lambda+a_3)(\lambda^3+\hat{a}_1\lambda^2+\hat{a}_2\lambda+\hat{a}_3)=0, \quad (27)$$

where a_1, a_2, a_3 are given by Eq. (22) and

$$\hat{a}_1=\frac{2}{9}\kappa^2[1-15b\gamma+10\gamma^2],$$

$$\hat{a}_2=\frac{8}{81}\kappa^4[4(\gamma^2-3b\gamma-2)(2\gamma^2+9b\gamma+17)+(64+18b^2+11\gamma^2+36b^2\gamma^2+69b\gamma+\gamma^4-3b\gamma^3)],$$

$$\hat{a}_3=\frac{32}{9}\kappa^4(1+b^2)(2+\gamma^2)(1-pC). \quad (28)$$

The boundary $\lambda=0$ is equivalent to conditions $a_3=0$ or $\hat{a}_3=0$, that is, to conditions $pC=2$ or $pC=1$. The latter condition is equivalent to conditions $c=-b\pm 3\sqrt{1+b^2}$. For $1-pC<0$ it holds $\hat{a}_3<0$ therefore at least one of the eigenvalues λ is positive. For $1-pC>0$ it holds $\hat{a}_3>0$ and hence $\lambda<0$. Thus the two-pulse solution is unstable for $1-pC<0$ and stable for $1-pC>0$ and $C=C_-$, and this is opposite to the stability of the single-pulse solution, at least if we do not consider the possibility of the oscillatory instability.

4. Stability of mixed-mode solutions

For $\alpha=1$ it holds $pC=1$, therefore, the stationary value of C reduces to $C=1/p$. The condition $\alpha=1$ is equivalent to conditions $c=-b\pm 3\sqrt{1+b^2}$. For the upper branch $c=-b+3\sqrt{1+b^2}$, the stationary value of γ reduces to $\gamma=b+\sqrt{1+b^2}$, and for the lower branch, $c=-b-3\sqrt{1+b^2}$, it follows $\gamma=b-\sqrt{1+b^2}$. It follows also that the stationary value of κ satisfies a condition $\kappa^2=C^2/(1+b\gamma)$.

For the investigation of stability of mixed-mode solutions we linearized the system (19) around the solution (C,κ,γ) for A_1 and around (C_2,κ_2,γ), for A_2, with C, κ, γ described above and $\kappa_2^2=C_2^2/(1+b\gamma)$. The obtained characteristic equation is as follows:

$$\lambda(\lambda^2+\tilde{a}_1\lambda+\tilde{a}_2)(\lambda^3+a_1\lambda^2+a_2\lambda+a_3)=0, \quad (29)$$

where

$$\tilde{a}_1=\frac{1}{9}\kappa_2^2(5\gamma^2+17), \quad \tilde{a}_2=-\frac{32}{9}\kappa_2^4(1+b^2)b\gamma, \quad (30)$$

and a_1, a_2, a_3 are given by Eq. (22). For $pC=1$ it holds $a_1>0$ and $a_3>0$. Hence, the stability boundary $\lambda=0$ is equivalent to a condition $b=0$.

In the case $\alpha=1$ the condition $a_2>0$ is fulfilled for $p^2>32\,\mathrm{sgn}(\gamma)b\sqrt{1+b^2}/(13\gamma^2+25)$. For $c=-b+3\sqrt{1+b^2}$ it holds that $\gamma>0$ and therefore $a_2>0$ for all values of p if $b<0$. For $c=-b-3\sqrt{1+b^2}$ it holds that $\gamma<0$ and therefore $a_2>0$ for all values of p if $b>0$. Next, the coefficient $\tilde{a}_2$ is positive for $b<0$ on the upper branch and for $b>0$ on the lower branch. Thus, the mixed-mode solution is stable for $b<0$ on the upper branch of $\alpha=1$ and for $b>0$ on the lower branch, and unstable otherwise.

5. Nonlinear dynamics produced by monotonic instabilities of a pulse solution

We have performed numerical simulations based on the variational model (19) for the points depicted on the Fig. 2. In accordance with the prediction of the linear theory, in region I, $\{-b-3\sqrt{b^2+1}<c<-b+3\sqrt{b^2+1}\}$, the only stable state corresponds to a single-pulse solution. This observation coincides also with that obtained in Ref. [21] by means of the direct numerical simulations of the original Eq. (1). An example of the transient evolution of the dynamical system (19) for point A_1 is shown in Fig. 3(a). The pulse with higher amplitude survives and tends to its stationary shape, while

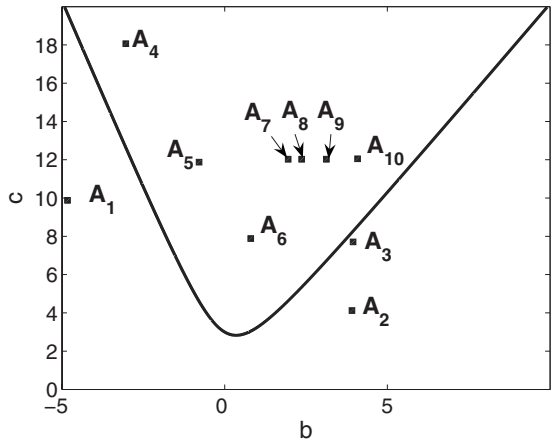

FIG. 2. Monotonic instability boundary $1-pC=0$ in the upper half of the (b,c) plane.

the pulse with lower amplitude decays. The same dynamics is observed in points A_2 and A_3.

In region II, $\{c<-b-3\sqrt{b^2+1}\}\cup\{c>-b+3\sqrt{b^2+1}\}$, the single-soliton solution is unstable with respect to the development of the second soliton. However, we observe two qualitatively different two-soliton regimes. Near the left boundary of region II (points A_4, A_5, A_6, and A_7) the stationary two-pulse state is observed, see Fig. 3(b) (for point A_4) and Fig. 4(a) (for point A_7). Near the right boundary of region II (points A_9 and A_{10}) the system tends to an oscillatory regime with alternating pulses [see Figs. 4(c) and 4(d)]. The boundary between two regimes is the oscillatory instability boundary of a two-pulse solution [see Fig. 4(b)], which depends on p and can be obtained numerically (see Fig. 5).

Numerical simulations (Fig. 6) show the supercritical character of the Hopf bifurcation on the oscillatory instability boundary of the two-pulse solution. Phase diagrams for the oscillating regime for the point A_{10} shown in Fig. 7 demonstrate a perfect periodicity and symmetry of oscillations.

For the investigation of evolution of behavior of a two-pulse solution we have fixed arbitrary values of the parameters c and p, $c=12$ and $p=5$, and looked at the changes of regimes for the changes of value of b, see Fig. 4. The periods of the oscillations increase with the approaching to the boundary of region II, see Fig. 8(a).

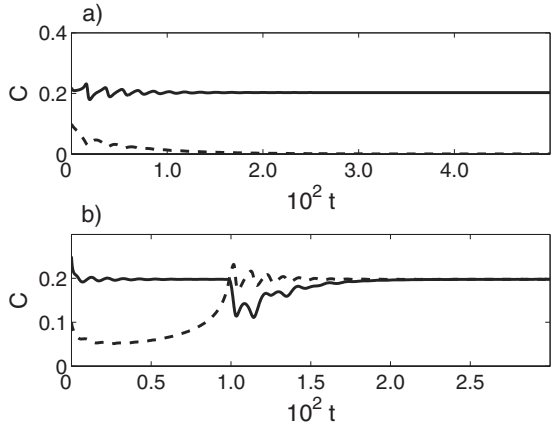

FIG. 3. Regimes for points (a) $A_1(-5,10)$, (b) $A_4(-3,18)$ and $p=5$. Solid line: $C_1(t)$, dashed line: $C_2(t)$.

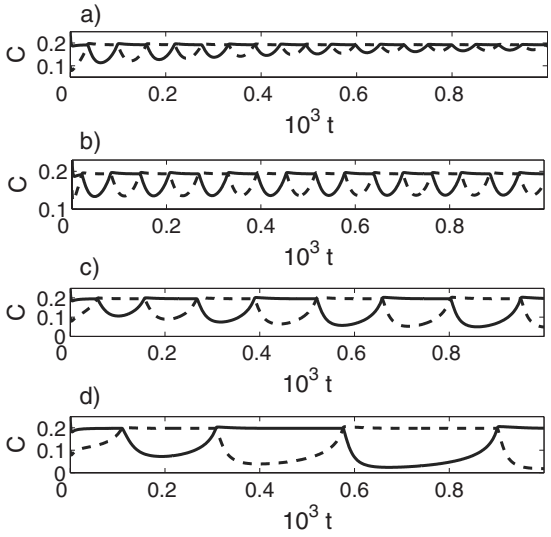

FIG. 4. Evolution of regimes for $p=5$ and points (a) $A_7(2,12)$, (b) $A_8(2.22,12)$, (c) $A_9(3,12)$, (d) $A_{10}(4,12)$. Solid line: $C_1(t)$, dashed line: $C_2(t)$.

Next, we have performed some calculations for the points near the right boundary of region II, b_*, that are presented in Table I. The behavior of the solution for small $b_*-b=\varepsilon$ can be understood in the following way.

Note, that in the whole region II the stationary values (C,κ,γ) determined by Eq. (6) satisfy the relations

$$2b<\gamma<c \tag{31}$$

and

$$\frac{\gamma-2b}{c-\gamma}=\frac{C^2}{\kappa^2(1+\gamma^2)}. \tag{32}$$

After the "revolution" when $C_1(t)$ becomes larger than $C_2(t)$, the variables $C_1(t)$, $\kappa_1(t)$, and $\gamma_1(t)$ rapidly relax to their stationary values (C,κ,γ) determined by Eq. (6), while $C_2(t)$ and $\kappa_2(t)$ strongly decrease. The decrease of $C_2(t)$ is more

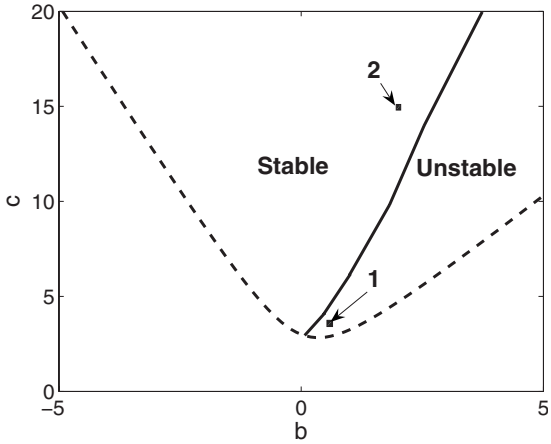

FIG. 5. Hopf bifurcation boundary (solid line) for $p=5$. The dashed line is the monotonic instability boundary $1-pC=0$. Comparison with a direct numerical simulation of CGLE. Point 1: competing pulses, point 2: chaotic pulses.

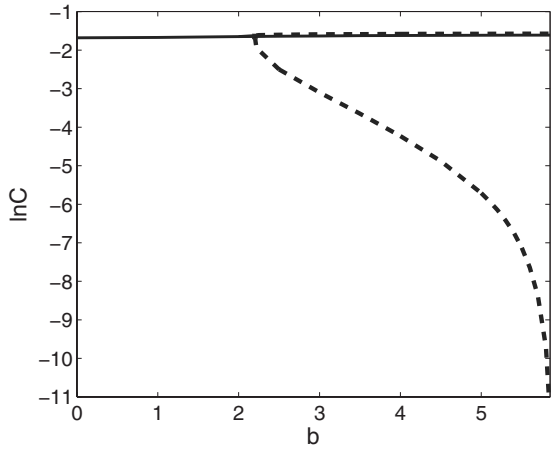

FIG. 6. Stationary and oscillatory regimes for $c=12$ and $p=5$. Solid line: stationary value of C, dashed lines: maximum and minimum values of C for an oscillating solution.

drastic than that of $\kappa_2(t)$, hence $C_2^2(t)$ becomes much smaller than $\kappa_2^2(t)[1+\gamma_2^2(t)]$ [see Fig. 8(e)]. According to Eqs. (19) and (32), γ_2 tends to a quasistationary value $2b<\gamma$ [see Fig. 8(c)]. During a long interval of time $C_2(t)$ grows nearly exponentially, with the growth rate λ about $1-pC\sim\varepsilon$ [see Fig. 8(a)], while $\kappa_2(t)$ continues to decrease [see Fig. 8(d)]. Eventually, $C_2^2(t)$ becomes larger than $\kappa_2^2(t)[1+\gamma_2^2(t)]$ [see Fig. 8(e)], therefore γ_2 starts to grow tending to $c>\gamma$ [see Fig. 8(c)].

The exponential growth of $C_2(t)$ from its minimal value C_m to the point of "revolution" takes the time T_+ which is determined roughly by the relation $C_m\exp(\lambda T_+)=C$ (of course, the exponential growth is violated when C_2 becomes of the order of 1, but that stage is relatively short). Then $C_2(t)$ becomes larger than $C_1(t)\approx C$, thus on this stage $\max\{C_1,C_2\}=C_2(t)$ [see Fig. 8(b)]. Because of the enhanced strength of the feedback control, $C_1(t)$ starts to decay and becomes small. Decay of $C_1(t)$ continues, until $C_2(t)$, which approaches C from above, starts to satisfy the condition $1-pC_2(t)>0$. The time T_- between the "revolution" and the arriving to the minimum value of $C_1(t)=C_m$ is proportional to $1/\varepsilon$ (see Table I). Then the process is repeated. The stage of the exponential growth is the longest one, therefore the whole period $T=2(T_-+T_+)$ satisfies the relation $T\varepsilon\sim\ln(C_m)$ (see Table I).

In conclusion to this subsection, let us compare the predictions of the finite-dimensional model with the results of the direct numerical simulation of Eq. (1) [21]. The oscillatory regime with alternating pulses corresponds to the regime

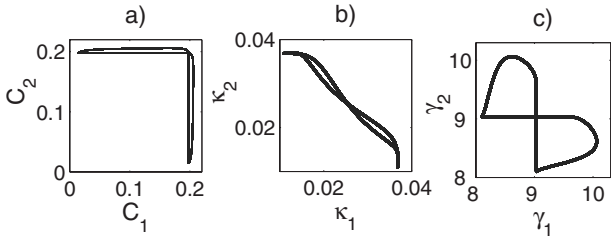

FIG. 7. Cycle loops for the point $A_{10}(4,12)$, $p=5$.

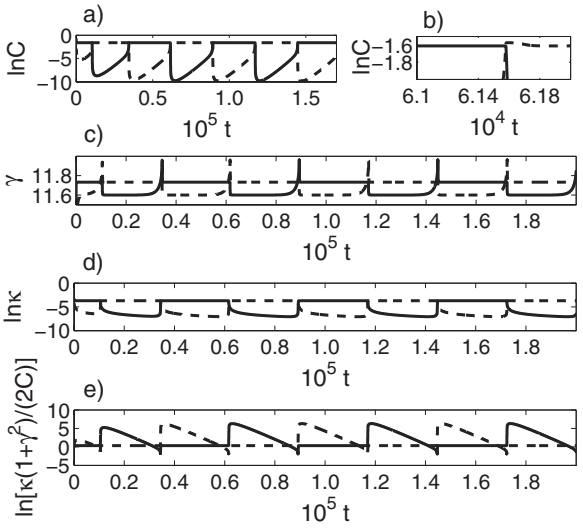

FIG. 8. Oscillations for point (5.8,12), $p=5$. Solid line: $C_1(t)$, dashed line: $C_2(t)$.

of "competing pulses" which is observed in numerics to the right from the boundary shown in Fig. 5 (point 1).

As to the regime of coexisting pulses, its basic counterpart in Ref. [21] is the regime of stationary multiple pulses. However, the model (19) predicts stationary coexisting pulses also in the regions where the multiple pulses are not fully stationary but coalesce from time to time, and the regime of chaotic pulses, where the multiple pulses are subject to some chaotic motion (point 2 in Fig. 5). The latter types of dynamics cannot be obtained in the framework of the model (19) which ignores the motion of pulses and is unable to describe the coalescence of pulses. Still, it explains the difference between multipulse regimes and regimes of competing pulses where there is only one pulse in the computation region, except some short transition periods.

C. Multipulse interactions

The generalization of the model to the case of arbitrary number of interacting pulses is straightforward. In the case of N pulses, we obtain the following system:

$$\dot{C}_j=\frac{1}{9}C_j[9-9p\ \max\{C_1,C_2,\ldots,C_N\}+8C_j^2-(\gamma_j^2+6b\gamma_j+7)\kappa_j^2],$$

$$\dot{\kappa}_j=\frac{4}{9}\kappa_j[C_j^2-(3b\gamma_j+2-\gamma_j^2)\kappa_j^2],$$

$$\dot{\gamma}_j=\frac{2}{3}C_j^2(c-\gamma_j)+\frac{2}{3}\kappa_j^2(2b-\gamma_j)(1+\gamma_j^2),\quad j=1,\ldots,N. \tag{33}$$

Region I (see Fig. 1) where one-pulse solutions can be observed is unchanged. In the left part of region II (see Fig. 1) one obtains stable stationary multipulse solutions (in agreement with the results of Ref. [30]); any initial disturbances

TABLE I. Behavior near the boundary for $c=12$, $p=5$; the value of $b_*=5.87321392113$.

	4.5	5	5.5	5.8	5.85
ε	1.373214	0.873214	0.373214	0.073214	0.023214
T	1298.72	2558.24	7906.8	55443.8	204297.4
$\ln(C_m)$	−4.8797	−5.708	−7.13	−9.7803	−11.6249
$\varepsilon T/\ln(C_m)$	−365.48	−391.36	−413.87	−415.04	−407.97
T_-	139	217	557	3040	9693
εT_-	190.88	189.49	207.88	222.57	225.01

decay after some transient process [see Fig. 9(a)]. With the growth of b, these solutions become oscillatory unstable; the instability leads to the development of time-periodic regimes characterized by alternation of pulses [see Fig. 9(b)]. A further growth of b leads to the appearance of more complicated scenarios of "revolution" where several pulses take part [Fig. 9(d)] and to the development of nonperiodic alternation regimes, that have, however, sufficiently long intervals of periodic alternation of pulses [Fig. 9(c)]. Alternations of several pulses with different location have been observed in direct numerical simulations [21].

D. Internal oscillations of pulses

1. Applicability of low-dimensional models for the description of radiating pulses

The possibility of the descriptions of oscillations by means of a variational approach was a subject of discussion since the time when it was applied to solitons governed by the one-dimensional nonlinear Schrödinger equation [26,31]. Indeed, the variational approach based on the approximation of the disturbance by a localized trial function of the same structure as the base soliton solution, predicts internal oscillations with a certain frequency. However, it is well known that the set of eigenfunctions for the nonlinear Schrödinger equation linearized around the soliton solution, does not include localized oscillatory internal modes [32]. The oscillatory eigenfunctions do not decay on the infinity, which means that an oscillating soliton always radiates. Therefore, the *Ansatz* used by the variational approach does not reproduce the shape of the eigenfunction sufficiently. The oscillations of the soliton take form of beating between soliton and the radiation waves [26], and its frequency differs from that predicted by the variational approach [31].

We can foresee a similar difficulty in the case of pulses governed by the controlled subcritical Ginzburg-Landau equation. Though in the case $\mu=1-pC<0$ the radiation decays and the oscillatory eigenfunctions are localized, their shape may be essentially different from that of the base solution, and hence it may be poorly approximated by the *Ansatz* (16). Note that the direct computation of the eigenfunctions for the linearized problem (1) carried out for $b=c=0$, has shown that the function $R(x)$ for eigenfunctions is a nonmonotonic function of x in each of regions $x>0$ and $x<0$ [33]. Therefore, we can expect that unlike the control-dominated dynamics described in Sec. IV B, which is determined mainly by the pulse amplitudes and is not sensitive to the details of the disturbance shape, the computation of intrinsic oscillations of solitons by means of the variational approach can be less precise.

In the present section, we consider internal oscillations of pulses, both by means of a finite-dimensional model and a direct numerical simulation. In order to check the predictions of the variational approach, we perform direct numerical simulations of pulse oscillations, and compare results of both approaches.

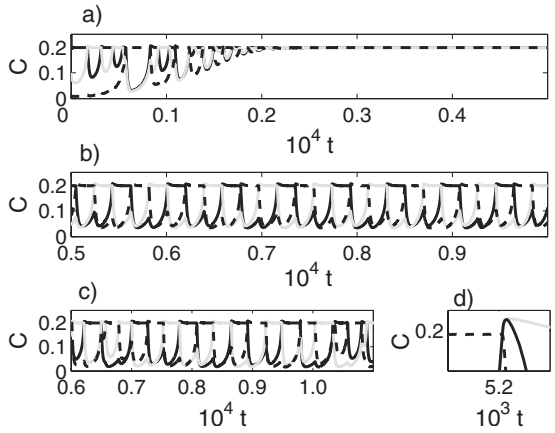

FIG. 9. Regimes for $N=3$ and $p=5$ for points (a) $b=0.03$, $c=4$; (b) $b=0.5$, $c=4$; (c) $b=0.7$, $c=4$; (d) a "revolution" for $b=0.7$, $c=4$. Black line: $C_1(t)$, gray line: $C_2(t)$, dashed line: $C_3(t)$.

2. Linear oscillatory instability of a pulse solution

In the framework of model (17), for $\lambda=i\omega$ it holds that $a_3=a_1\cdot a_2$. This boundary is obtained numerically, see Fig. 10.

However, for special values of b and c the oscillatory instability boundary can be obtained analytically. For example, for $b=-c$ it follows that $\gamma=0$, $C^2=2\kappa^2$, and $C=p\pm\sqrt{p^2-2}$. The coefficients of the characteristic Eq. (21) now have a simplified form

$$a_1=\frac{1}{9}[9pC+C^2],$$

$$a_2=\frac{2}{9}\kappa^2[17pC-16C^2+4c^2C^2],$$

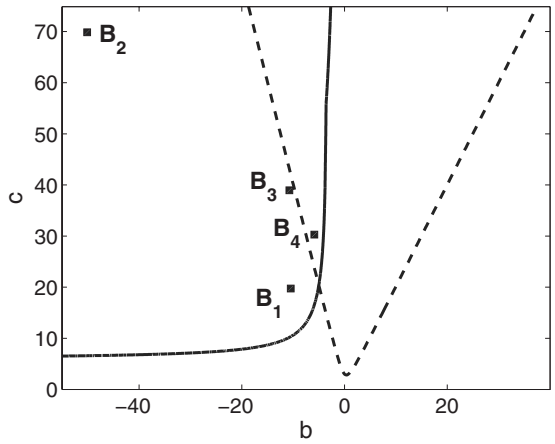

FIG. 10. Boundary of oscillatory instability (solid line) for $p=5$. The dashed line is the monotonic instability boundary $1-pC=0$.

$$a_3 = \frac{32}{9}\kappa^4(1+c^2)(2-pC). \tag{34}$$

For $\lambda = i\omega$ it holds $a_3 = a_1 \cdot a_2$ and therefore

$$c^2 = \frac{21p^2C^2 + 50pC - 224}{8(29p^2C^2 - 67pC + 38)}. \tag{35}$$

The minimum is reached in the point $p=2.0332$ and $c=4.9665$. For $p \to 1.6632$ it holds that $c \to \infty$, and for $p < 1.6632$ it holds that $c^2 < 0$.

3. Numerical simulation

In order to investigate the oscillatory behavior of pulse solutions, a computer test of the finite-dimensional model (19) was provided in points denoted in Fig. 10. The following possible regimes were obtained: (i) oscillations of a single-pulse solution (points B_1 and B_2), see Fig. 11; (ii) oscillations on the background of alternating pulses (point B_3), see Fig. 12(a); and (iii) oscillations of a two-pulse solution (point B_4), see Fig. 12(b).

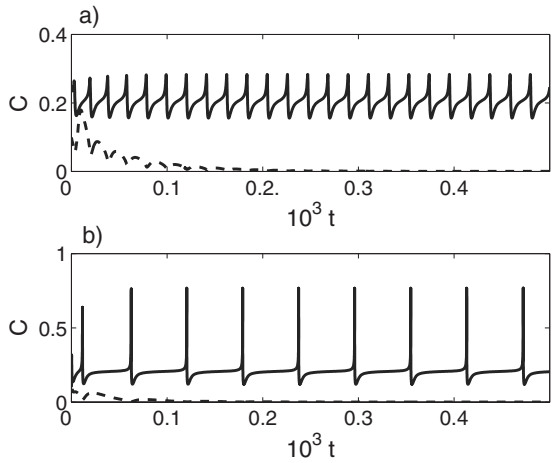

FIG. 11. One-pulse solution in points (a) $B_1(-10,20)$, (b) $B_2(-50,70)$, and $p=5$. Solid line: $C_1(t)$, dashed line: $C_2(t)$.

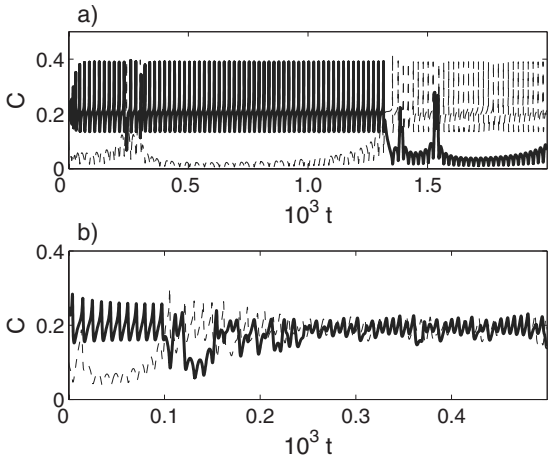

FIG. 12. (a) Alternating pulses in $B_3(-10,40)$, $p=5$; (b) two-pulse solution in $B_4(-5,30)$, $p=5$. Solid line: $C_1(t)$, dashed line: $C_2(t)$.

Next, a direct numerical simulation of Eq. (1), with the periodic boundary conditions, was held in order to obtain the same oscillatory regimes. We have not managed to obtain the regime of alternating oscillating pulses and the regime of a two-pulse oscillating solution. Oscillations of a one-pulse solution were obtained in the point B_2 [see Fig. 13(a)] for a certain length of the x-axis segment. However, the increase of the segment's length can lead to the disappearance of oscillations of a one-pulse solution. Therefore, we can conclude that the internal oscillations of pulses are observed only in a finite region.

The form of one-pulse solution is presented in Fig. 13(b). One can see that in addition to the pulse, the solution contains small-amplitude waves ("radiation") which persist due to periodic boundary conditions. Hence, the assumptions used by the construction of the finite-dimensional model, are poorly satisfied.

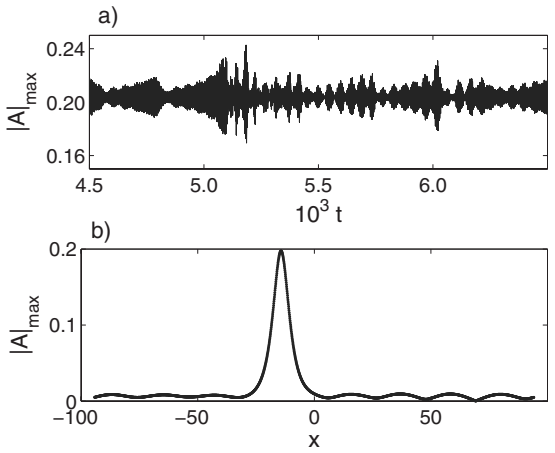

FIG. 13. Direct numerical simulation for point $B_2(-50,70)$ and $p=5$: (a) obtained oscillations; (b) the form of soliton.

V. CONCLUSIONS

Dynamics of subcritical oscillations under the action of a global feedback control has been considered. We have constructed a finite-dimensional model for the description of the indirect interaction of pulses stabilized by the active control.

In the framework of the model, we have explained and analyzed the transition from the stationary multipulse regime to the regime of alternating pulses. At the same time, the internal oscillations of pulses, which essentially depend on the interaction between the pulses and radiated waves, cannot be adequately described in the framework of the low-dimensional model.

ACKNOWLEDGMENTS

The support of the Israel Science Foundation (Grant No. 812/06), Technion V.P.R. fund, and Minerva Center for Nonlinear Physics of Complex Systems is acknowledged. The authors thank M.A. Zaks, A.A. Golovin, and B.A. Malomed for valuable discussions.

[1] J. Tang and H. H. Bau, Phys. Rev. Lett. **70**, 1795 (1993).
[2] L. E. Howle, Phys. Fluids **9**, 1861 (1997).
[3] H. H. Bau, Int. J. Heat Mass Transfer **42**, 1327 (1999).
[4] A. C. Or, R. E. Kelly, L. Cortelezzi, and J. L. Speyer, J. Fluid Mech. **387**, 321 (1999).
[5] A. C. Or and R. E. Kelly, J. Fluid Mech. **440**, 27 (2001).
[6] R. O. Grigoriev, Phys. Fluids **14**, 1895 (2002).
[7] R. O. Grigoriev, Phys. Fluids **15**, 1363 (2003).
[8] N. Garnier, R. O. Grigoriev, and M. F. Schatz, Phys. Rev. Lett. **91**, 054501 (2003).
[9] M. Bertram and A. S. Mikhailov, Phys. Rev. E **63**, 066102 (2001).
[10] M. Bertram and A. S. Mikhailov, Phys. Rev. E **67**, 036207 (2003).
[11] C. Beta, M. Bertram, A. S. Mikhailov, H. H. Rotermund, and G. Ertl, Phys. Rev. E **67**, 046224 (2003).
[12] A. S. Mikhailov and K. Showalter, Phys. Rep. **425**, 79 (2006).
[13] A. A. Nepomnyashchy, A. A. Golovin, V. Gubareva, and V. Panfilov, Physica D. **199**, 61 (2004).
[14] D. Battogtokh and A. Mikhailov, Physica D. **90**, 84 (1996).
[15] D. Battogtokh, A. Preusser, and A. Mikhailov, Physica D. **106**, 327 (1997).
[16] Y. Kawamura and Y. Kuramoto, Phys. Rev. E **69**, 016202 (2004).
[17] B. Echebarria and A. Karma, Chaos **12**, 923 (2002).
[18] K. A. Montgomery and M. Silber, Nonlinearity **17**(6), 2225 (2004).
[19] P. Kolodner and G. Flätgen, Phys. Rev. E **61**, 2519 (2000).
[20] C. Beta and A. S. Mikhailov, Physica D. **199**, 173 (2004).
[21] A. A. Golovin and A. A. Nepomnyashchy, Phys. Rev. E **73**, 046212 (2006).
[22] L. M. Hocking and K. Stewartson, Proc. R. Soc. London, Ser. A **326**, 289 (1972).
[23] N. R. Pereira and L. Stenflo, Phys. Fluids **20**, 1733 (1977).
[24] K. Nozaki and N. Bekki, J. Phys. Soc. Jpn. **53**, 1581 (1984).
[25] S. Popp, O. Stiler, E. Kuznetsov, and L. Kramer, Physica D **114**, 81 (1998).
[26] B. A. Malomed, Prog. Opt. **43**, 71 (2002).
[27] S. Chávez Cerda, S. B. Cavalcanti, and J. M. Hickmann, Eur. Phys. J. D **1**, 313 (1998).
[28] V. Skarka and N. B. Aleksić, Phys. Rev. Lett. **96**, 013903 (2006).
[29] E. N. Tsoy, A. Ankiewicz, and N. Akhmediev, Phys. Rev. E **73**, 036621 (2006).
[30] W. Schöpf and L. Kramer, Phys. Rev. Lett. **66**, 2316 (1991).
[31] E. A. Kuznetsov, A. V. Mikhailov, and I. A. Shimokhin, Physica D **87**, 201 (1995).
[32] D. J. Kaup, Phys. Rev. A **42**, 5689 (1990).
[33] B. Y. Rubinstein, A. A. Nepomnyashchy, and A. A. Golovin, Phys. Rev. E **75**, 046213 (2007).